Part 1

Experimental setup: Collider, detector and algorithms

1.1 The Large Hadron Collider

The Large Hadron Collider (LHC) [1, 2] is a particle accelerator installed in the former LEP [3] tunnel at CERN [4]. It is 26.7 km in circumference and consists out of two separate rings, which are, in periods of operation, inhabited by two counter-circulating beams. At the interaction points of the two beams, either proton-proton collisions or heavy ion collisions take place. In this thesis, only collision data from the year 2012 is analysed. Thus all machine values cited in the following chapters and paragraphs refer to the setup in 2012 (if not stated otherwise).

The beams are separated into bunches which rotate with a bunch spacing of 50 ns corresponding to a collision frequency of 20 MHz. Before the bunches are actually filled into the LHC rings they are pre-accelerated in other accelerators, which are (in the order they are actually passed by the protons) Linac2, Proton Synchrotron Booster (PSB), Proton Synchrotron (PS), Super Proton Synchrotron (SPS). The injector chain and the LHC ring with its experiments is visualised in Fig 1.1.1.

In the LHC, the beams are kept on the circuit with the help of a magnetic field of 4.76 T. Further quadrupole and sextupole magnets squeeze and focus the bunches. They have a spread of roughly 8 cm length and a Gaussian shape radius of 20 μm RMS at the
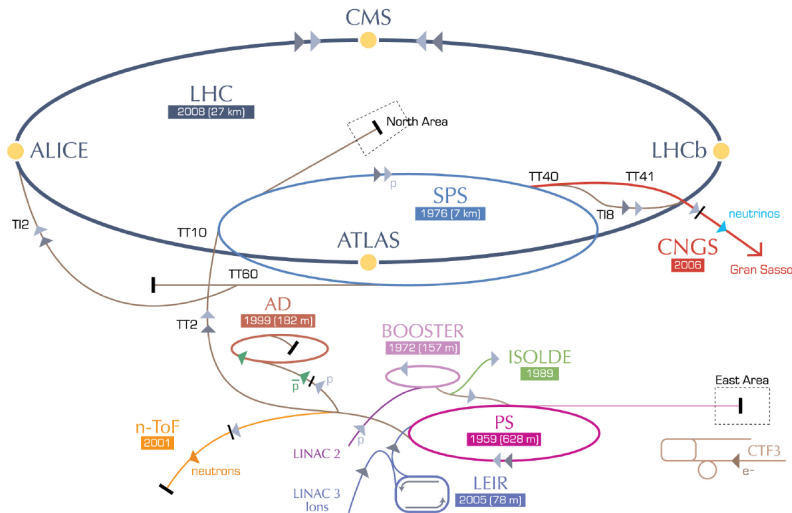

Figure 1.1.1: Visualisation of the LHC with its experiments and the injector chain. Taken from [5].

interaction point. The number of contained protons in each bunch is of the order 10^{11}. The LHC has eight different insertion region, where four of them are dedicated to the four main experiments of the LHC, the CMS, ATLAS, LHCb and ALICE experiments. The CMS [6,7] and ATLAS [8–10] experiments are so-called "general purpose experiments", not designed for one specific task. In contrary, the LHCb [11] and the ALICE [12] experiment are designed with an emphasis on CP-violation measurements and heavy ion collisions, respectively. Each experiment is interested thus in different processes to happen at the beam collision points. The number of expected event for a given process can be expressed in terms of the corresponding cross section σ times the integrated luminosity.

$$N = L \cdot \sigma, \tag{1.1.1}$$

with an integrated luminosity of $L = \int \mathcal{L} \, dt$, where $\mathcal{L}$ is the instantaneous luminosity (which can change over time).

The instantaneous luminosity $\mathcal{L}$ depends on the several machine parameters, such as the collision frequency f, the number of particles in the bunches n_1 and n_2, the spread in the transverse plane of the bunches σ_x and σ_y and a geometrical correction parameter F due to the crossing angle of the two bunches at the interaction point

$$\mathcal{L} = \frac{f n_1 n_2}{4\pi \sigma_x \sigma_y} \cdot F. \tag{1.1.2}$$

In 2012, the peak luminosity was $7.7 \cdot 10^{33} \frac{1}{\mathrm{cm}^2\,\mathrm{s}}$. The total integrated luminosity over time recorded at the CMS experiment is shown in Fig. 1.1.2.
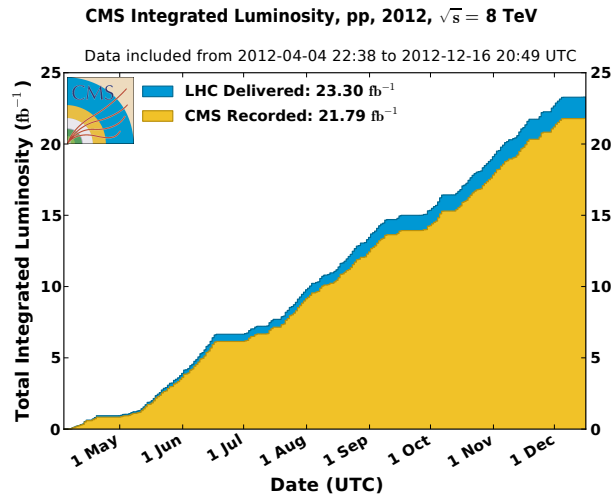

Figure 1.1.2: Integrated luminosity delivered by LHC (blue) and recorded by CMS (orange) in the year 2012. Taken from [13].

1.2 CMS detector

The Compact Muon Solenoid (CMS) detector [6,7] is a general purpose detector, designed to explore particle physics phenomena up to the multi-TeV scale. The detector concept is an onion-like structure of different layers, each one made up with a different type of detector. In Fig. 1.2.1, a perspective view of the CMS detector is depicted. The used coordinate system at the CMS experiment consists of the pseudorapidity $\eta = -\ln \tan \frac{\theta}{2}$ and the azimuthal angle ϕ. The advantage of the pseudorapidity η is the Lorentz invariance with respect to the z-axis (beam axis). The angle ϕ covers the direction in the $x - y$ plane (orthogonal to the beam axis).

In the following, the various detector components of the CMS detector from the inside to the outside will be explained. In order to ensure a possible measurement of the first detector component, a magnetic field is needed in order to bend the particles' trajectories.
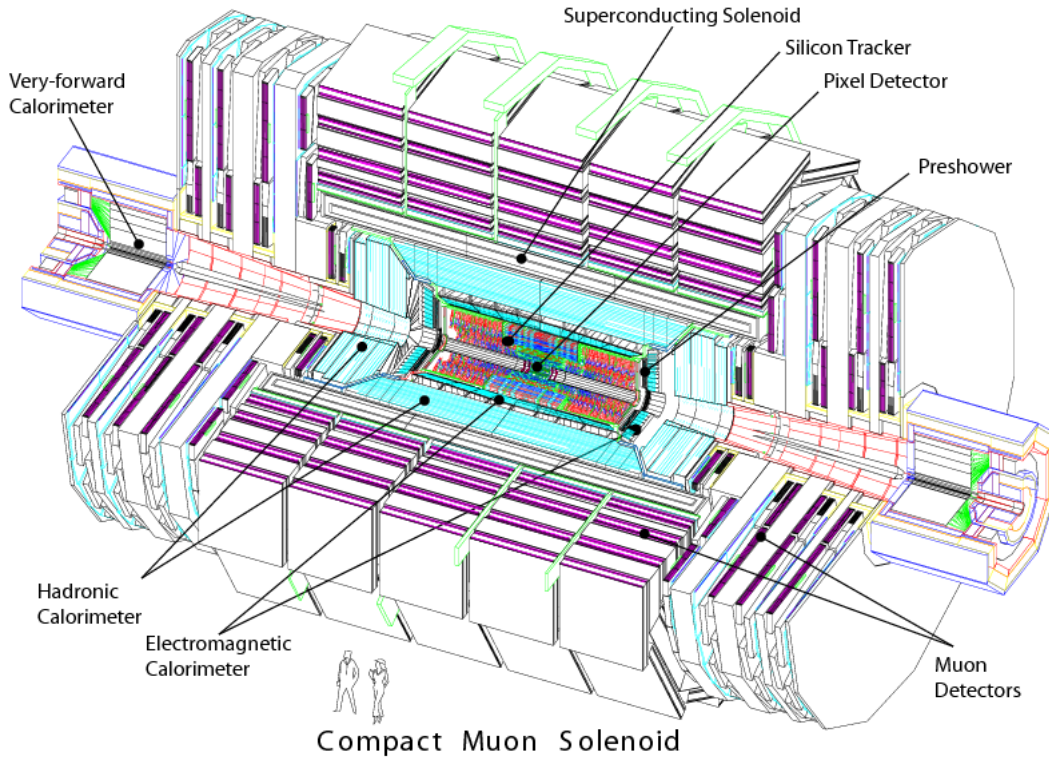

Figure 1.2.1: A perspective view of the CMS detector. Taken from [6]

50 At the CMS experiment, this magnet is lcoated between the hadron calorimeetr and the
51 muon chmabers. it is vxxx return yokes and further bla.

1.2.1 The tracking system

53 The tracking detector [14,15] is the innermost detector of the CMS experiment. It is a sili-
54 con semiconductor detector and is included for the tasks of vertex and track reconstruction
55 by the measurement of particle's energy losses. Additionally, the energy measurements
56 can be used for measuring a particle's dE/dx. A schematic sketch of the tracker at CMS
57 is depicted in Fig. 1.2.2. The tracking system is devided into parts using different tech-
58 nologies. First, a silicon pixel detector and second, a silicon strip detector. How both are
59 constructed, will be explained in the following two sections. As a calibration of the silicon
60 pixel detector was performed within this PhD thesis (see Section **??**), an emphasis will be
61 put on the pixel detector.

The silicon pixel tracker

63 The silicon pixel detector consists of three different cylindrical layers in the barrel region
64 (at radii of $4.4\,\text{cm}$, $7.3\,\text{cm}$ and $10.2\,\text{cm}$) and two discs in the encaps (at z-distances of
65 $34.5\,\text{cm}$ and $46.5\,\text{cm}$) (cf. Fig. 1.2.2). It is made up of 1440 modules in total (barrel +
66 endcap), each module containing 8 or 16 read-out-chips (ROCs). Each read-out-chip is
67 bumb bonded [**?**] to a pixel system of 52×80 pixels, that are read out in double columns.
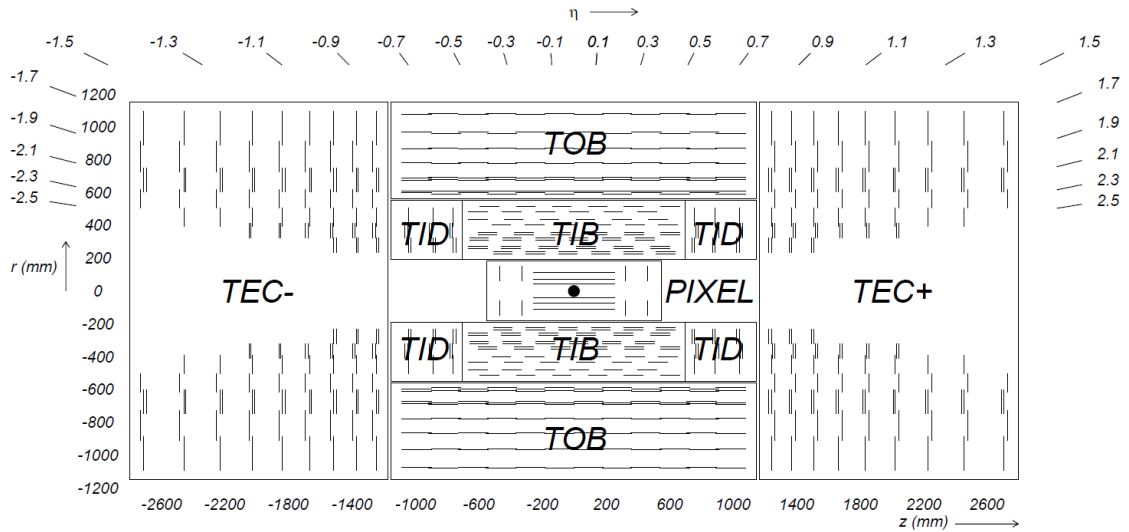68 A visualisation of the pixel system is shown in Fig. 1.2.3.

Figure 1.2.2: Schematic sketch of the silicon tracker at CMS in the $z - \phi$ plane. Taken
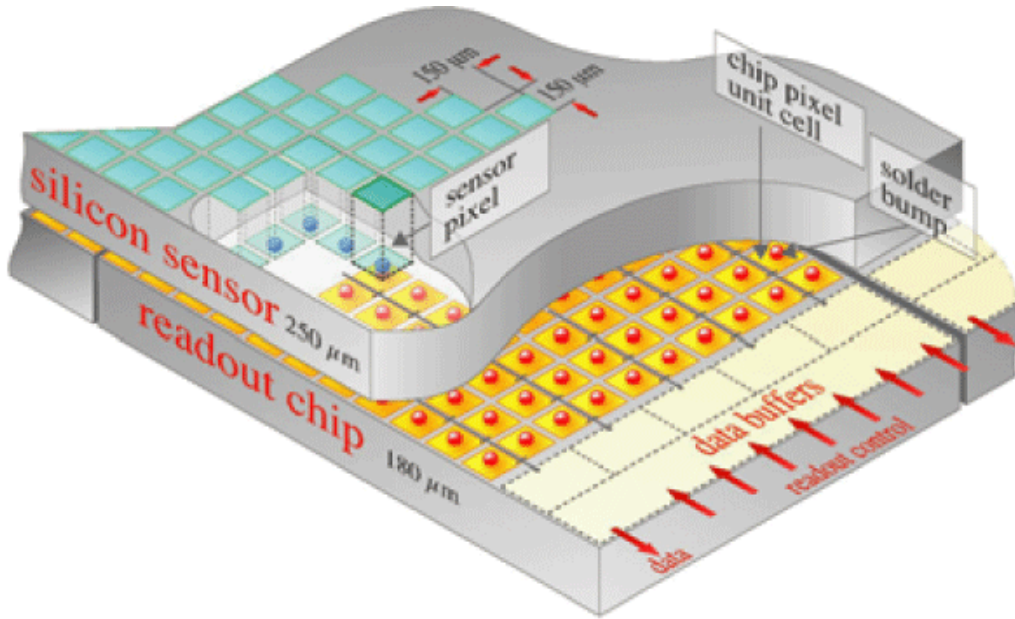from [16].

Figure 1.2.3: Schematic sketch of a part of a silicon pixel tracker module icnluding the silicon sensors and the read-out-chip (ROC). Taken from [16].

The silicon pixel detector is very important for the reconstruction of primary and secondary vertices as well as the reconstruction of particles' tracks. Therefore a high spatial resolution is needed. This is achieved by the small size of the pixels ($150 \times 100 \, \mu$m^2) and the exploitation of the spread of the energy deposition across several pixels (in average the energy is deposited across 2-4 pixels FIXME). Exploting this spread across pixels, a spatial resolution of $13 \times 14 \, \mu$m^2 in the barrel region and $10 \times 17 \, \mu$m^2 in the encaps can be achieved [**?**]. The high spatial resolution makes the pixel detector perfectly suited for the reconstruction of vertices.

The silicon strip tracker

The silicon strip tracker is the next to innermost detector of the CMS experiment. It is devided into strips

Energy measurements in the tracking system

1.2.2 The calorimeters

The electromagnet calorimeter

The Hadronic calorimeter

1.2.3 The muon system

1.2.4 The magnet

1.2.5 The trigger system

- General purpose detector (picture) - short overview (tarcker, calorimeters, etc), pseudorapittyt and phi and z

- Tracker (Pixel tracker - silicon strip tracker - energy measurements in the tracker)

- Calorimeter - eCAL and HCAL

- Muon system

- Trigger system

- 10 pages

1.3 Event reconstruction and particle identification

Event reconstruction relies on very complicated algorthms bla

1.4 Event simulation

Bibliography

[1] L. Evans and P. Bryant, "LHC Machine", *JINST* **3** (2008) S08001.
`doi:10.1088/1748-0221/3/08/S08001`.

[2] O. S. Bruning, P. Collier, P. Lebrun et al., "LHC Design Report Vol.1: The LHC
Main Ring", *Technical Design Report* **CERN-2004-003** (2004).

[3] "LEP Design Report: Vol.2. The LEP Main Ring",.

[4] CERN, "CERN, public web page". `www.cern.ch`. Accessed: 2016-01-17.

[5] CERN, "LHC: the guide", *CERN Brochure* **CERN-Brochure-2009-003-Eng**
(2009).

[6] CMS Collaboration, "The CMS experiment at the CERN LHC", *JINST* **3** (2008)
S08004. `doi:10.1088/1748-0221/3/08/S08004`.

[7] CMS Collaboration, "CMS physics: Technical design report", *Technical Design
Report* **CERN-LHCC-2006-001, CMS-TDR-008-1** (2006).

[8] ATLAS Collaboration, "The ATLAS Experiment at the CERN Large Hadron
Collider", *JINST* **3** (2008) S08003. `doi:10.1088/1748-0221/3/08/S08003`.

[9] ATLAS Collaboration, "ATLAS: Detector and physics performance technical design
report. Volume 1", *Technical Design Report*
CERN-LHCC-99-14,ATLAS-TDR-14 (1999).

[10] ATLAS Collaboration, "ATLAS: Detector and physics performance technical design
report. Volume 2", *Technical Design Report* **CERN-LHCC-99-15,
ATLAS-TDR-15** (1999).

[11] LHCb Collaboration, "The LHCb Detector at the LHC", *JINST* **3** (2008) S08005.
`doi:10.1088/1748-0221/3/08/S08005`.

[12] ALICE Collaboration, "The ALICE experiment at the CERN LHC", *JINST* **3**
(2008) S08002. `doi:10.1088/1748-0221/3/08/S08002`.

[13] CMS Collaboration, "CMS Luminosity - Public Results", *Public CMS Wiki* (2015).
https://twiki.cern.ch/twiki/bin/view/CMSPublic/LumiPublicResults, Topic
revision: r111.

[14] CMS Collaboration, "The CMS tracker system project: Technical Design Report",
     Technical Design Report **CERN-LHCC-98-006,CMS-TDR-5** (1997).

[15] CMS Collaboration, "The CMS tracker : addendum to the Technical Design
     Report", *Technical Design Report* **CERN-LHCC-2000-016** (2000).

[16] CMS Collaboration, "Description and performance of track and primary-vertex
     reconstruction with the CMS tracker", *JINST* **9** (2014), no. 10, P10009,
     `arXiv:1405.6569`. `doi:10.1088/1748-0221/9/10/P10009`.